Arch. Metall. Mater. **67** (2022), 2, 465-470

DOI: https://doi.org/10.24425/amm.2022.137778

M.H. AZMI[1], M.Z. HASNOL[1], M.F.A. ZAHARUDDIN[1*], S. SHARIF[1], S. RHEE[2]

EFFECT OF TOOL PIN PROFILE ON FRICTION STIR WELDING OF DISSIMILAR MATERIALS AA5083 AND AA7075 ALUMINIUM ALLOY

Friction stir welding (FSW) currently contributes a significant joining process for welding aluminium, magnesium, and other metals in which no molten or liquid state were involved. It is well known that aluminium alloys are more effective, promising for different applications light weight, strength and low cost. This study aims to determine how such tools geometry and tool speed can be related to dissimilar material in the joining process. Specifically, it investigates whether the distribution of the weld zone particularly between tool pin profile to rotational speed. In this context, the influence of tool pin profile and tool rotational speed in relation to the mechanical properties and microstructure of friction stir welded. The aim of this study is also to test the hypothesis that better mixing between dissimilar metals at higher tool rotational speed along the weld path. Three different tool profiles were configured with AA5083 and AA7075. During welding, notable presence of various types of defects such as voids and wormholes in the weld region. The results of this work showed that the tool pin profile and weld parameter are significant in determining mechanical properties at different tool rotational speed. The highest tensile strength achieved was about 263 MPa and the defect-free joint was obtained by using the threaded tapered cylindrical pin tool at a rotational speed of 800 rpm. These findings indicate that different tool profiles influence differently on the formation of defects at welds. On this basis, the tool geometry should be considered when designing experimental friction stir welded joint.

Keywords: Friction stir welding; aluminium alloys; tool pin; mechanical properties

1. Introduction

Friction stir welding is a solid-state welding process that yields welds of good quality for materials that are difficult to be weld for instance aluminium [1,2]. Generally, this technique is done in solid-state without melting the material. The material to be joined does not melt and recast. The heat required is produced by rubbing between the base material and the tool that moves along between the materials to be joined while rotating at a certain speed. This welding technique is considered comparatively as a new joining process which was invented by The Welding Institute in 1991. This joining procedure has also been used in joining other materials for instance thermoplastics [3,4], steel [5], and composites [6,7]. This demonstrates its vast possibility of welding materials that are hard to be joined through welding. Frictional heat is produced in this procedure using a non-consumable rotating tool. The rotating tool causes local changes in the welded material due to the heat generated and mechanical deformation [8]. The Welding Institute, TWI in 1998 did a study on aluminium tailored blanks for door panels and they have also shown new ideas on FSW drive shafts including space frames. This project involved BMW, Ford, Volvo, and few other automotive companies [9]. Since then, more and more automotive companies around the world have employed friction stir welding techniques in their production. Various studies have been done on investigating the effects of different tool pin profile on friction stir welding. In a study done by [10], various tools with different pin profiles have been used to understand the effect of tool pin profile and tool shoulder diameter on friction stir processed (FSP) zone formation in AA6061 aluminium alloy.

2. Experimental procedure

The material for the workpiece are AA7075 and AA5083 aluminium alloys. AA7075 is widely used in various applications due to its favourable characteristics such as high resistance towards corrosion due to seawater and atmospheric condition. AA5083 also shows good corrosion resistance towards seawater. The plates to be joined were in the dimension

[1] UNIVERSITI TEKNOLOGI MALAYSIA, SCHOOL OF MECHANICAL ENGINEERING, FACULTY OF ENGINEERING, 81310 JOHOR BAHRU JOHOR, MALAYSIA
[2] HANYANG UNIVERSITY, DEPARTMENT OF MECHANICAL ENGINEERING, 17 HAENGDANG-DONG, SEONGDONG-GU, SEOUL 133-791, KOREA

* Corresponding author: faridh@utm.my

of 250 mm (L) × 50 mm (W) × 6.35 mm (T). TABLE 1 shows the chemical composition, TABLE 2 presented the physical properties, and TABLE 3 highlighted the mechanical properties of both AA5083 and AA7075.

Design of Experiment Setup

The experiments were designed with 3^k factorial design. In this study, 3^2 design was applied. The 3^2 design is the simplest three-level design where it has two factors, each at three levels. The two factors are the tool pin profiles; threaded straight cylindrical, tapered cylindrical, and threaded tapered cylindrical, and the tool rotational speed; 600, 700, and 800 rpm. TABLE 4 shows the experimental design with different parameter setup. The traverse speed is kept constant at 40 mm/min.

The specimens used for the FSW processing experiments were machined from AA5083 and AA7075 plates. The FSW process were done on a vertical Milling Machine (Refer Fig. 1). The tool was fabricated from H13 steel and used for single-pass friction stir butt joint welding. The plates (to be welded) were fixed onto the machine table using strap clamps. 4 clamps were used to hold the plates down at the edges. 2 more strap clamps were put at the sides of the plates to ensure the plates does not move apart during FSW process. The fixture of the plates is as shown in Fig. 2.

In this study, two factors, each with three levels; tool rotational speed and tool pin profiles were studied. The tool is plunged in between the materials manually with a depth of 6 mm. Once the pin is fully plunged and the shoulder is in contact with the plates, the machine table is moved 40 mm/min along the welding line. The rotating tool is moved at 100 mm to form a weld of the same distance. Once the 100 mm distance of tool travel was achieved, the table was stopped, and the tool

TABLE 1

Chemical Composition of AA5083 & AA7075

Element %	Mg	Mn	Cr	Fe	Si	Zn	Ti	Cu	Others	Remainder
Alloy (5083)	4.00-4.90	0.40-1.00	0.05-0.25	0.40 (Max)	0.40 (Max)	0.25 (Max)	0.15 (Max)	0.10 (Max)	0.05 (Max) each 0.15 (Max) total	Aluminium
Alloy (7075)	2.10-2.90	0.30	0.18-0.28	0.50 (Max)	0.40 (Max)	5.10-6.10 (Max)	0.20 (Max)	1.2-2.0 (Max)	0.05 (Max) each 0.15 (Max) total	Aluminium

TABLE 2

Physical Properties of AA5083 & AA7075

Property	Density	Melting Point	Modulus of Elasticity	Thermal Conductivity	Electrical Resistivity
Value Alloy (5083)	2.65 g/cm^3	570°C	72 GPa	121 W / m.K	0.058×10^{-6} Ω .m
Alloy (7075)	2.81 g/cm^3	477-635°C	71.7 GPa	130 W / m.K	0.052×10^{-6} Ω .m

TABLE 3

Mechanical Properties of AA5083 & AA7075

Property	Yield Strength	Tensile Strength	Hardness Vickers
Value Alloy (5083)	215 MPa	323 Mpa	70 Hv
Alloy (7075)	503 MPa	570 MPa	132 Hv

TABLE 4

Process Parameter

Symbol	Process Parameter	Units	Level 1	Level 2	Level 3
A	Rotation Speed	rev/min	600	700	800
B	Tool Geometry		Threaded straight cylindrical (TSC)	Tapered cylindrical (TC)	Threaded tapered cylindrical (TTC)

TABLE 5

Experimental Design

Std.	Factor 1 A: Rotation Speed rev/min	Factor 2 B: Tool Geometry
1	600	TSC
2	600	TC
3	600	TTC
4	700	TSC
5	700	TC
6	700	TTC
7	800	TSC
8	800	TC
9	800	TTC

Fig. 1. Vertical milling machine

Fig. 2. Workpiece clamped onto the machine table

was pulled out of the welded plated while rotating. The machine was only shut after the tool has been pulled out completely. The tool pin length for every tool geometry design is kept constant at 6 mm. The tool pin profiles is shown in Fig. 3.

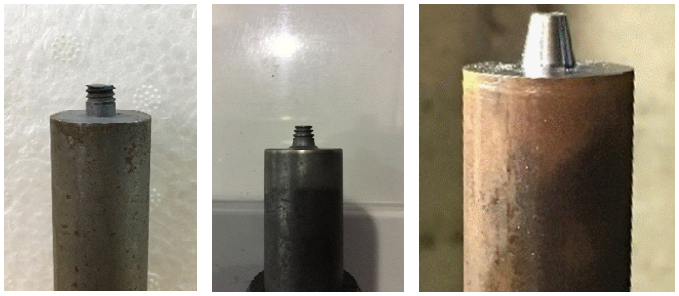

a) b) c)

Fig. 3. FSW tools geometry (a) Threaded straight cylindrical, (b) Threaded tapered cylindrical, (c) Tapered cylindrical

A total of nine weld joints are made with dissimilar AA7075 and AA5083. Specimens for tensile testing are prepared as per the ASTM E8 standards. The tensile test are carried out on the Instron 5982 universal testing machine and the hardness test is carried out by Vickers hardness test. The sample of the tensile test and the hardness test is shown in Fig. 4.

Fig. 4. Tensile test sample

3. Results and discussions

The results consist of visual inspection on the weld surface, hardness distribution, and tensile testing. The top view of the welded joint is as shown in TABLE 6.

TABLE 6

Top view on the weld line

(a) 600 rpm, TSC	(b) 700 rpm, TSC	(c) 800 rpm, TSC
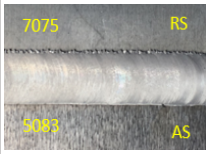	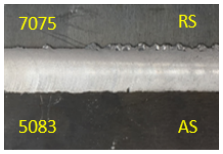	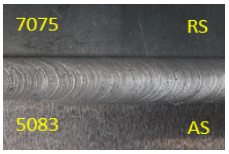
(d)) 600 rpm, TC	(e)) 700 rpm, TC	(f)) 800 rpm, TC
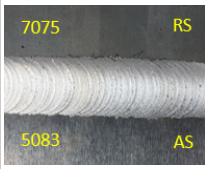	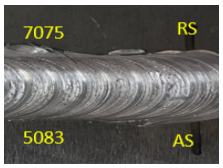	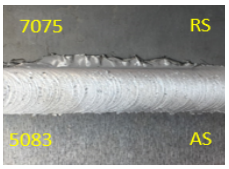
(g)) 600 rpm, TTC	(h)) 700 rpm, TTC	(i)) 800 rpm, TTC
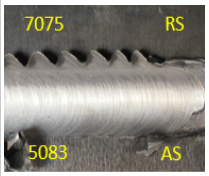	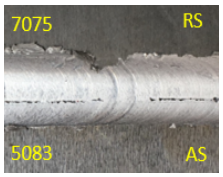	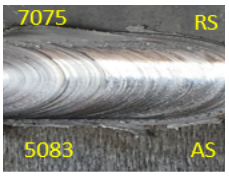

Nine (9) welded specimens were visually inspected to identify any defects formed at the welded surface of dissimilar materials. Specimens (a), (b), and (c) made by using a threaded straight cylindrical tool, shows smooth welded surface with no excessive flash formed. Specimens (e) and (f) show some flash formed at the retreating side of AA7075. This shows that the heat input is high causing the tool to produce more excessive flash. It was discovered that at 600 rpm using threaded tapered cylindrical tool, excessive flash formed on the surface of both advancing and retreating side. Tunnel defects are formed when 700 rpm is used for the threaded tapered cylindrical tool. This was due to the low heat input generated by the FSW tool.

TABLE 7 shows the macrostructure of FSW welds. Sample (a), (b), and (c) shows the formation of tunnel/void defects at the mid-bottom part of the stir zone (SZ) and thermomechanical affected zone (TMAZ). The formation of tunnel/void defect was due to the low heat input and improper mixing of materials. The largest tunnel defect can be seen when 700 rpm was applied using TSC tool. The macrostructure also shows the formation of friction stir onion ring pattern due to the process of friction heating produced by rotation of the tool and the traverse movement which extrudes the softened metal around the retreating side of the tool [11].

TABLE 7

Macrostructure of FSW welds

(a) 600 rpm, TSC	(b) 700 rpm, TSC	(c) 800 rpm, TSC
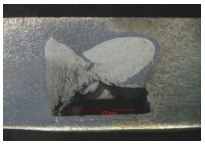	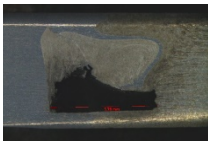	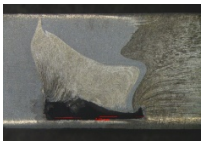
(d) 600 rpm, TC	(e) 700 rpm, TC	(f) 800 rpm, TSC
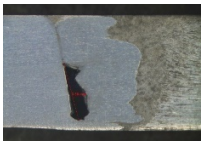		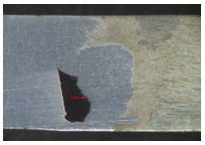
(g) 600 rpm, TTC	(h) 700 rpm, TTC	(i) 800 rpm, TSC
		

For FSW specimen by TC tool, it can be observed that for every sample, tunnel/void were formed at the stir zone of AA5083 side. The pictures also show that when using this tool, the mixing of materials was lesser compared to other tools. Kissing bond (as shown in Fig. 5) defects can also be seen at 600 and 700 rpm. TTC tool produced welds with relatively smaller tunnel defect with a defect-free joint at 800 rpm tool rotational speed. The formation of tunnel/void defect was due to the low heat input and improper mixing of materials. The pictures also show that by using this tool, the mixing of materials was better compared to other tools.

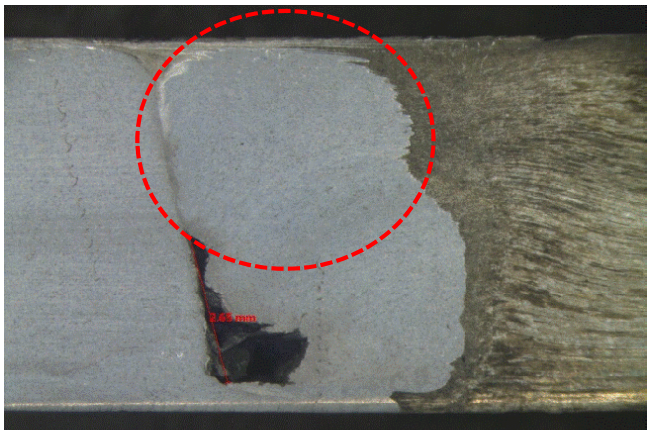

Fig. 5. Kissing bond defect (circled)

At the advancing side of AA5083, the hardness increases as it approaches the weld centre when using threaded tools (TSC & TTC) as shown in Fig. 5 & Fig. 7. This shows that threaded tool provides better mixing of materials as the higher hardness value indicates the movement of AA7075 into the advancing side.

Based on Fig. 9, the highest tool rotational speed used which was at 800 rpm, produced friction stir welded joints with the highest ultimate tensile stress. At low speed, it can be observed that the UTS obtained was fairly similar ranging from 124 MPa to 144 MPa. Due to the absence of defects for instance tunnel defect and kissing bond, welded joint using TTC tool at 800 rpm achieved the highest ultimate tensile strength at 263 MPa among all other welds. The lowest UTS was recorded at specimens where severe defects were formed which significantly weakened the welded joint.

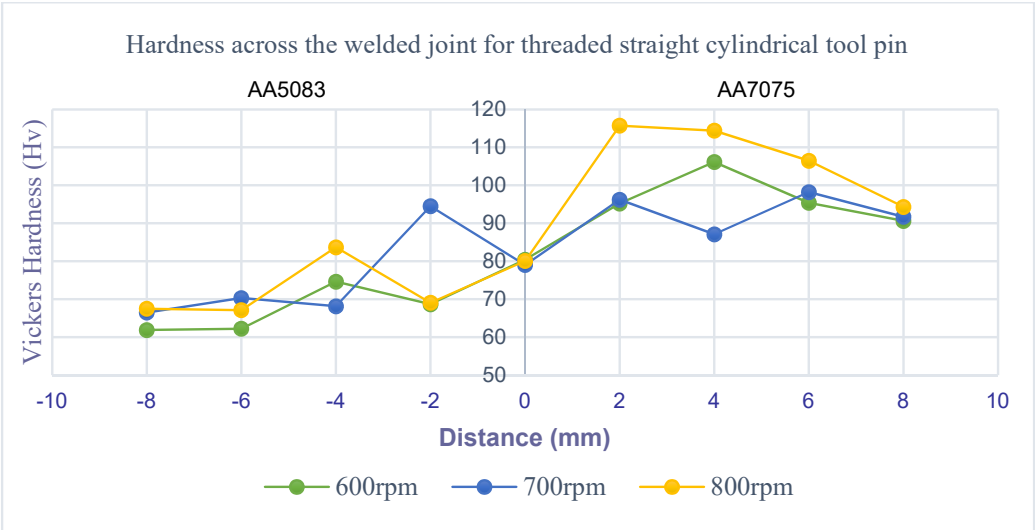

Fig. 6. Hardness distribution using TSC tool

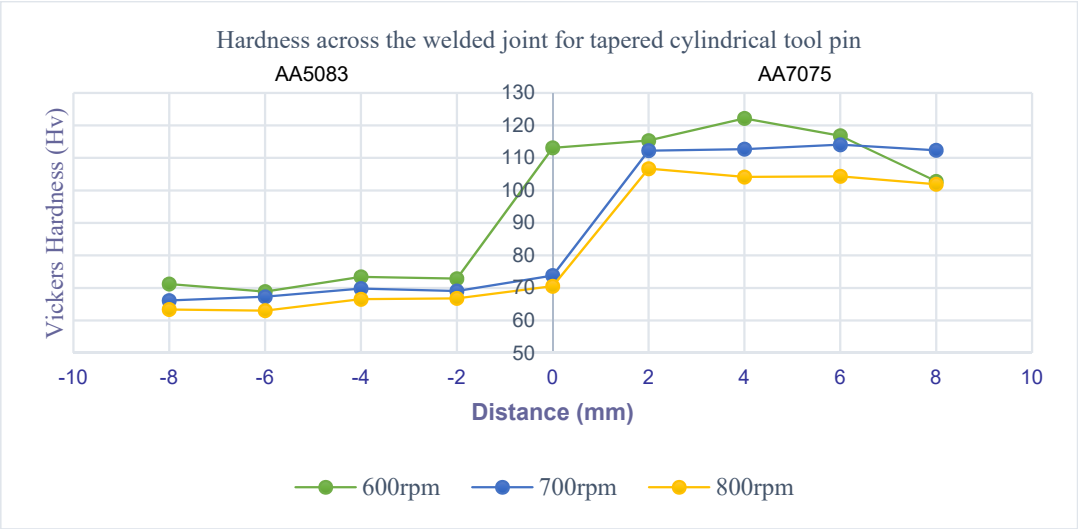

Fig. 7. Hardness distribution using TC tool

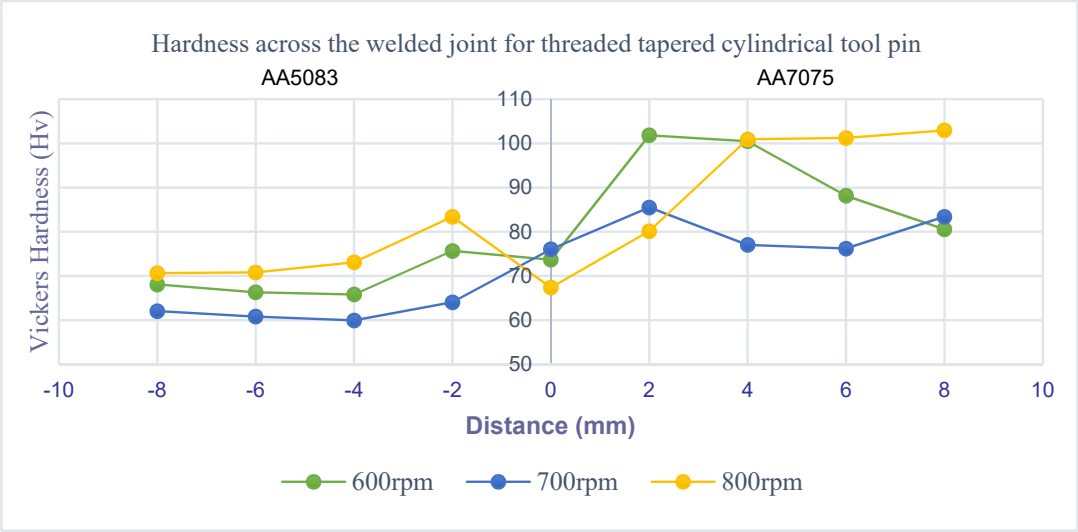

Fig. 8. Hardness distribution using TTC tool

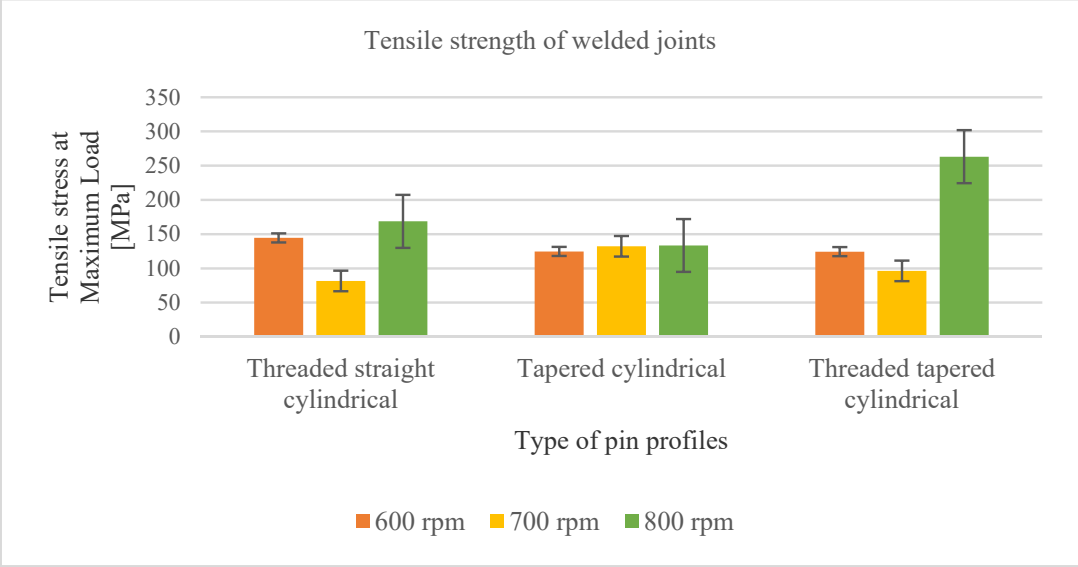

Fig. 9. Tensile strength of weld joints for each tool and speed

4. Conclusions

Different tool profiles influence differently on the formation of defects at welds. For threaded straight cylindrical, the tunnel defect formed at the mid-bottom part of the stir zone, and the size is relatively bigger while for tapered cylindrical tool, the void formed at the stir zone of AA5083 and the size is smaller. The kissing bond can also be observed with less mixing of dissimilar materials in the friction stir welded zone. For threaded tapered cylindrical tools, the size of the tunnel defect is much smaller, however at 700 rpm, tunnel defect formed on top of the welds. This was due to the lack of heat generated at the tool. All in all, threaded tools provide better material flow as there is an increase in hardness at the advancing side of welds. Threaded tapered cylindrical produced joints have the highest tensile strength and better mixing based on the hardness distribution. The higher tool rotational speed produce friction stirs welded joint with higher tensile strengths. The welded joint was also defect free.

Acknowledgments

This material is based upon work supported by the Ministry of Higher Education (MOHE), Malaysia and Research Management Centre of UTM for the financial support through the RUG funding, Q.J130000.3551.06G76.

REFERENCES

[1] M. Aissani, S. Gachi, F. Boubenider, Y. Benkedda, Materials and Manufacturing Processes, **25** (11), 1199-1205 (2010). DOI: https://doi.org/10.1080/10426910903536733

[2] M.S. Srinivasa Rao, B.V.R. Ravi Kumar, M. Manzoor Hussain, Materials Today: Proceedings **4** (2), 1394-1404 (2017). DOI: https://doi.org/10.1016/j.matpr.2017.01.161 .

[3] S. Inaniwa, Y. Kurabe, Y. Miyashita, H. Hori, Proceedings of the 1st International Joint Symposium on Joining and Welding 137-142 (2013). DOI: https://doi.org/10.1533/978-1-78242-164-1.137

[4] S. Eslami, T. Ramos, P.J. Tavares, P.M.G.P. Moreira, Procedia Engineering **114**, 199-207 (2015). DOI: https://doi.org/10.1016/j.proeng.2015.08.059

[5] V.C. Shunmugasamy, B. Mansoor, G. Ayoub, R. Hamade, Journal of Materials Engineering and Performance **27** (4), 1673-1684 (2018). DOI: https://doi.org/10.1007/s11665-018-3280-3

[6] C. Devanathan, A.S. Babu, Procedia Materials Science **6**, 1470-1475 (2014). DOI: https://doi.org/10.1016/j.mspro.2014.07.126

[7] S. Madhavarao, C.R.B. Raju, G.S.V.S. Kumar, Materials Today: Proceedings **5** (2), 7735-7742 (2018). DOI: https://doi.org/10.1016/j.matpr.2017.11.450

[8] M.J. Starink, A. Deschamps, S.C. Wang, Scripta Materialia **58** (5), 377-382 (2008). DOI: https://doi.org/10.1016/j.scriptamat.2007.09.061

[9] W.M. Thomas, S.W. Kallee, D.G. Staines, P.J. Oakley, Friction Stir Welding – Process Variants and Developments in the Automotive Industry. SAE Technical Paper Series (2006). DOI: https://doi.org/10.4271/2006-01-0555

[10] K. Elangovan, V. Balasubramanian, Materials & Design **29** (2), 362-373 (2008). DOI: https://doi.org/10.1016/j.matdes.2007.01.030

[11] Z.W. Chen, S. Cui, Scripta Materialia **58** (5), 417-420 (2008). DOI: https://doi.org/10.1016/j.scriptamat.2007.10.026